Liquefaction Assessment in Gravels using Vs and DPT Blow count from Case Histories

KYLE ROLLINS, PROFESSOR, BRIGHAM YOUNG UNIVERSITY AND JASHOD ROY, GEOTECHNICAL ENGINEER, KIEWIT ENGINEERING

ABSTRACT

Gravelly soils have liquefied at multiple sites in at least 27 earthquakes over the past 130 years. These gravels typically contain more than 25% sand which lowers the permeability and makes them susceptible to liquefaction. Typical Standard Penetration Tests (SPT)- or Cone Penetration Test (CPT_-based correlations can be affected by large gravel particles and lead to erroneous results. To deal with these problems, we have developed liquefaction triggering curves for gravelly soils based on (1) shear wave velocity (V_s) and (2) a 74-mm diameter dynamic cone penetrometer (DPT), less affected by gravel particles. These correlations are based on case histories where gravelly soils did and did not liquefy in past earthquakes. The new probabilistic triggering curves reduce the range between 15 and 85% probability of liquefaction in comparison to previously developed curves. The V_s-based liquefaction triggering curves for gravels shift to the right relative to similar curves based on sands. Good agreement has been obtained with liquefaction factor of safety computed by the DPT and Becker penetration tests (BPT) at sites in Idaho subjected to the 1985 M_w 6.9 Borah Peak earthquake.

I. INTRODUCTION

Liquefaction of loose saturated granular soils results in significant damage to civil infrastructure such as dams, bridges, roadways, pipelines, and ports in nearly every earthquake. Liquefaction and the resulting loss of shear strength can lead to landslides, lateral spreading, loss of vertical and lateral bearing support for foundations, and excessive foundation settlement and rotation. Direct and indirect economic losses resulting from liquefaction are substantial costs to society. A significant number of gravel liquefaction case histories have occurred during more than 27 earthquake events over the past 130 years. Assessing the potential for liquefaction of gravelly soils in a reliable, cost-effective manner has always posed a great challenge for geotechnical engineers. Liquefaction assessment is particularly important for older dams that were constructed on gravelly soil foundations or with poorly compacted gravel shells before the potential for liquefaction in gravels was recognized. Likewise, many ports around the world were constructed of gravelly soils or rockfill which was believed to be immune to liquefaction. For these projects, assessing the potential for liquefaction and determining appropriate remedial measures can become multi-million-dollar decisions. These decisions involve both life-safety and regional economic issues. Over the past 15 years, gravel liquefaction has caused significant damage to ports in Greece, Chile, Ecuador, and New Zealand. In addition to these large projects, gravel liquefaction must be routinely considered for a myriad of small to medium projects throughout the world.

Early numerical modeling by Seed et al. [1] found that excess pore pressure generated by an earthquake would dissipate as fast as they generated if the hydraulic conductivity of the gravel was greater than about 0.3 centimeters per second (cm/s). This suggested that clean gravels would be unlikely to liquefy. The range of grain size distribution curves for gravels that have liquefied in field case histories is plotted in Fig.1 [2]. Although gravel contents often exceed 50%, they are typically well-graded sandy gravels with more than 30% sand. Roy and Rollins [2] found that these sandy gravels typically had hydraulic conductivities less than 0. 3 cm/s because the sand filling the void space between the gravel particles was reducing the hydraulic conductivity of the mixture. This allows excess pore pressures to generate during earthquake shaking.

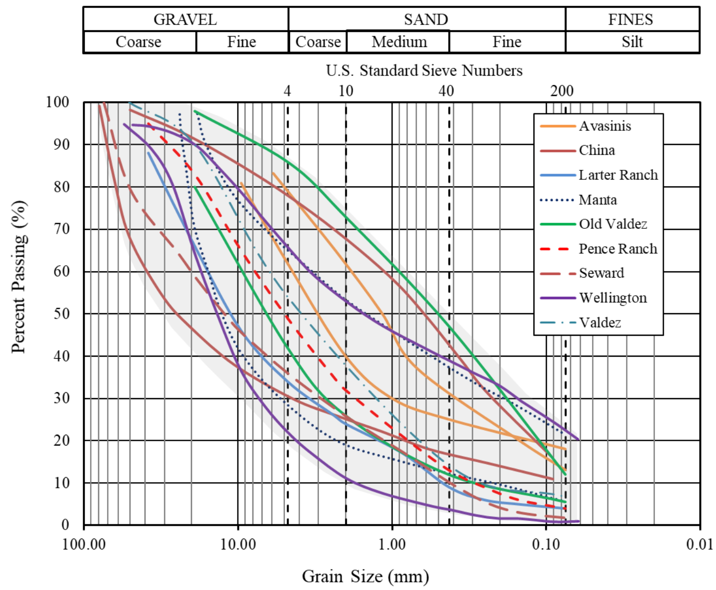

Figure 1. Grain-size distribution curves for gravelly soils that have liquefied in field case histories [2].

II. PENTRATION TEST METHODS

Typical laboratory investigation techniques have generally proven to be ineffective for characterizing gravelly soil due to the cost and difficulty of extracting undisturbed sample from gravelly deposits using freezing techniques [3]. In addition, the large particle size of gravels can lead to artificially high penetration resistance values from traditional in situ tests such as the cone penetrometer (CPT) test and the Standard Penetration (SPT) test [4]. The 168 millimeter (mm) diiameter Becker Penetration Test (BPT) [5, 6] reduces the potential for artificially high penetration values; however, this method is relatively expensive and is not available outside of North America. In addition, the method requires a correlation between the BPT blow count and the SPT blow count which leads to greater uncertainty relative to methods that are directly correlated with field liquefaction resistance.

As another approach for gravelly soils, Chinese engineers in the Chengdu region, faced with widespread gravel deposits, developed a Dynamic Cone Penetrometer (DPT) with a 74-millimeter (mm) or 3 inch diameter cone tip for site characterization. The methodology is a large-size implementation of the lightweight dynamic cone penetrometer that is used extensively for assessment of compaction of soils in pavement applications [7] and different cone geometries are also known as dynamic probing in Europe [8]. In the Chinese version of the DPT, the cone tip is driven continuously with a 120 kilogram (kg) hammer dropped from one meter (equivalent to 340 pound weight dropped from 30 inches) and is capable of penetrating medium to dense gravel and cobbles. DPT soundings can be easily performed with conventional SPT drilling rigs or even simple tripod systems, making it viable worldwide. In contrast to the straight sides of the BPT, the cone tip tapers back to a 60 mm drill rod to reduce rod friction. At 74 mm, the DPT diameter is 50% larger than the SPT and 110% larger than a standard 10 cm^2 CPT; however, it is still 55% smaller than the BPT. Although the BPT provides the largest diameter to particle size ratio of all tests, the DPT is superior to the SPT or CPT and could be a reasonable solution in many cases depending on the gravel size and percentage.

Based on field case histories of gravel liquefaction in the M_w 7.9 Wenchuan earthquake, Cao et al. [3] developed probabilistic liquefaction triggering curves for gravels based on the DPT blow count. However, these curves are based on relatively few data points from one earthquake and a geologic environment [3]. Because of the limited number of data points and the possibility of false negatives (sites where liquefaction may have occurred but did not produce surface manifestation), the individual triggering curves (85 to 15% probability of liquefaction) are spread over a large range. In contrast, more mature probabilistic liquefaction triggering curves for sands based on the CPT [9] have more closely grouped probability curves because of the larger size of the data set. In addition, the Cao et al. [3] triggering curves were developed for a single event of *Mw* 7.9 without incorporating any correction to the seismic demand by using the Magnitude Scaling Factor (*MSF*). Thus, applicability of these curves would become questionable for evaluating the liquefaction potential of gravelly soils for other seismic events of different Magnitude. Although existing *MSF* models developed for sand liquefaction [10] can be used, it is unclear whether they are appropriate for gravel liquefaction using the DPT.

Therefore, it becomes crucial to add more case histories to the DPT database with different earthquake magnitudes and geologic settings to develop an improved DPT-based liquefaction triggering procedure and a gravel-based MSF curve.

III. SHEAR WAVE VELOCITY METOHDS

As an alternative to penetration resistance testing, in-situ measurement of shear wave velocity (V_s) is a popular way of characterizing the liquefaction resistance of soil deposits. V_s is a basic mechanical property of soil materials, directly related to the small strain shear modulus (G_0), that has been used to evaluate liquefaction resistance in sand. The use of V_s as a field index of liquefaction resistance is soundly based on the fact that both V_s and liquefaction resistance are similarly, but not proportionally, influenced by void ratio, effective confining stresses, stress history and geologic age [10]. In addition, V_s is considerably less sensitive to the problems of soil compression and reduced penetration resistance when fines are present, compared with SPT and CPT methods. Moreover, V_s requires only minor corrections for fines content (*FC*) at least for sands [11]. The primary advantage of the in-situ V_s approach is that testing can be performed at sites where borings are not possible, or the penetration test results may be unreliable. Hence, V_s measurement can be considered as a reliable and economical alternative to overcome the difficulties of penetration testing within gravelly strata.

The traditional methods of measuring V_s requires a penetrometer or an instrumented borehole to measure the travel time of shear waves at various depths. A downhole test requires one borehole to measure the vertically propagating wave, while a cross-hole test requires at least two boreholes to directly measure the horizontally propagating wave [12]. These invasive test methods are usually quite expensive owing to the cost of drilling, casing, and grouting boreholes. In the last two decades, some advanced non-invasive test methods (Spectral Analysis of Surface Waves (SASW) and Multichannel Analysis of Surface Wave (MASW) have been developed, which indirectly define the V_s through the surface wave dispersion characteristics of the ground [12, 13, 14]. These non-invasive test methods have significantly reduced the cost of in-situ V_s estimation and made soil exploration possible at sites where penetration is not possible or economically feasible.

Although the Andrus and Stokoe [13] V_s-based liquefaction triggering curves for sand contained some gravel case histories, no liquefaction triggering curves based exclusively on gravel performance were available until recently [15]. SPT-V_s correlations developed by Ohta and Goto [16] for sands and similar correlations by Rollins et al. [17] for gravelly soils suggest that gravel profiles with higher shear wave velocities might still be susceptible to liquefaction than would be predicted by triggering curves based on sand.

After collecting a database of gravel case histories from the 2008 Wenchuan earthquake, Cao et al. [18] developed probabilistic liquefaction triggering curves for gravels based on Vs using logistic regression techniques However, these curves were based on only 47 data points (19 liquefaction and 28 no liquefaction points) that refer to a single earthquake and a similar geological environment [18]. Because of the limited number of data points and the possibility of false negatives (sites where liquefaction may have occurred but did not produce surface manifestation), the individual triggering curves (15% to 85%) widely separated as was the case for the DPT case histories. In contrast, V_s-based probabilistic liquefaction triggering curves for sands [11] have more closely grouped probability curves because of the larger size of the data set. Moreover, the Cao et al. [18] triggering curves were developed for a single event of M_w 7.9 without proposing any correction to the seismic demand for different earthquake magnitudes. Thus, it becomes difficult to use these curves for other magnitude events without using a Magnitude Scaling Factor developed for sand liquefaction [10]. Therefore, additional effort was necessary to collect more V_s data from the gravel liquefaction sites to improve the existing V_s-based liquefaction triggering curves for gravelly soils.

IV. COLLECTION OF ADDITIONAL FIELD CASE HISTORY DATA

In the present study, a larger database consisting of 174 V_s data points and 137 DPT data points has been compiled by collecting additional data points from seven different countries around the world where gravel liquefaction did or did not take place in 17 major earthquake events and adding them to the existing data points from China [3, 19]. Case histories with no liquefaction in Italy, Greece, and New Zealand were strategically identified, tested, and then added to the database to help constrain the position of the liquefaction triggering curves. For each case history, the cyclic stress ratio (CSR) has been obtained by using the simplified equation,

$$CSR = 0.65\ (a_{max}/g)\ (\sigma_{vo}/\ \sigma'_{vo})\ r_d \tag{1}$$

originally developed by Seed and Idriss [20] where a_{max} is the peak ground acceleration, σ_{vo} is the initial vertical total stress, σ'_{vo} is the initial vertical effective stress, and the r_d value in Eq. 1 was updated to include the effect of both depth and earthquake magnitude using the equation,

$$r_d = e^{[\alpha(z)+\beta(z)M_w]} \tag{2}$$

where:

$$\alpha(z) = -1.012 - 1.126 sin(^{z}/_{11.73} + 5.133) \tag{3}$$

$$\beta(z) = 0.106 + 0.118 sin(^{z}/_{11.28} + 5.142) \tag{4}$$

and z is the depth in meters, based on the work by Golezorkhi [21] and Idriss [22].

Peak ground accelerations *(PGA or a_{max})* for every location were taken from the literature or from USGS Shake Maps [23] where necessary as employed by Idriss and Boulanger [24] for their CPT database. Besides *CSR*, the moment magnitude (M_w) has been considered as another independent seismic variable for obtaining the liquefaction potential of gravelly soils. Values of M_w were found from available references regarding the appropriate earthquake. The data set contains a wide distribution of M_w ranging from 5.3 to 9.2 as well as *PGA* ranging from 0.17 to 0.6 g.

A. DPT Blow Count Corrections

The DPT blow count, N_{120}, represents the number of hammer blows to drive the penetrometer 30 cm deep with a 120 kg hammer dropped from a height of 1 m. Raw blow counts are typically reported at every 10 cm penetration but are multiplied by three to get the equivalent N_{120} for 30 cm of penetration. Based on 1200 hammer energy measurements, Cao et al. [25] found that the Chinese DPT provided an average of 89% of the theoretical free-fall energy. Since the energy delivered by a given hammer (E_{Hammer}) was different than the energy actually supplied by a Chinese DPT hammer ($E_{Chinese\ DPT}$), it was sometimes necessary to correct the measured blow count. In this study, the correction was made using the simple linear adjustment ratio suggested by Seed et al. [26] for SPT testing

$$N_{120} = N_{Hammer}\left(\frac{E_{Hammer}}{E_{Chinese\ DPT}}\right) \tag{5}$$

where N_{Hammer} is the number of blows per 0.3 m of penetration obtained with a hammer delivering an energy of E_{Hammer}. In addition, Cao et al. [1] recommend an overburden correction factor, C_n, to obtain the normalized N'_{120} value using the equation

$$N'_{120} = N_{120}C_n \tag{6}$$

Where,

$$C_n = \left(\frac{100}{\sigma'_{v0}}\right)^{0.5} \leq 1.7 \tag{7}$$

and σ'_o is the initial vertical effective stress in kN/m^2. In the current study, a limiting value of 1.7 was added to be consistent with the C_n used to correct penetration resistance from other in-situ tests [10]. For each case history a critical layer was selected below the water table and with the lowest ratio of blow count divided by CSR over at least one meter. All the critical liquefaction layers were located at depths less than about 14 m which is consistent with other liquefaction case history databases and with blow counts typically less than about 20.

B. Shear Wave Velocity Corrections

The V_s values obtained by various in-situ methods were corrected for overburden pressure to obtain V_{s1} using the equation:

$$V_{S1} = V_S \left(\frac{P_a}{\sigma'_{v0}}\right)^{0.25} \tag{8}$$

where σ'_{vo} is the initial vertical effective stress, and P_a is atmospheric pressure approximated by a value of 100 kPa as suggested by Sykora [26] and adopted by Youd et al. [10]. These normalized V_{s1} profiles based on the V_s testing were then plotted as a function of depth and a critical depth with the lowest average ratio of V_{s1}/CSR over a length of at least one meter. Once again, the critical layers based on V_{s1} were all shallower than 14 m.

V. DEVELOPMENT OF PROBABILISTIC TRIGGERING CURVES

Using the expanded database, a new set of probabilistic liquefaction triggering curves has been developed by logistic regression analysis based on V_{s1} and on N'_{120}. The triggering equations developed in the present study include the earthquake magnitude as an independent variable.

A. Probabilistic DPT-Based Liquefaction Triggering Curves

The logistical regression analysis was carried out using M_w, N'_{120}, and Ln(*CSR*) as independent variables and the following equation was developed to calculated the Cyclic Resistance Ratio (CRR)

$$CRR = exp\left[\frac{1.32M_w - 0.0008{N'}^3_{120} - \ln\left(\frac{1-P_L}{P_L}\right)}{5.2}\right] \tag{9}$$

where P_L is the probability of liquefaction expressed as a fraction. If a given probability and M_w of 7.5 is used in Eq. 9, a plot of *CRR* vs. N'_{120} can be produced for a given probability. Fig. 2 provides a plot of *CRR* vs. N'_{120} for M_w 7.5 for various P_L values. CSR and N'_{120} data points for each liquefaction and no liquefaction case history are also shown in Fig. 2 relative to the triggering curves proposed by Rollins et al. [28].

B. Probabilistic V_s-Based Liquefaction Triggering Curves

Logistical regression analysis was also carried out using M_w, V_{s1} and Ln(*CSR*) as independent variables and the following equation was developed to calculate the Cyclic Resistance Ratio (CRR)

$$CRR = exp\left[\frac{1.438M_w - 3.8x10^{-7}{V_{s1}}^3 - \ln\left(\frac{1-P_L}{P_L}\right)}{4.026}\right] \tag{10}$$

where P_L is the probability of liquefaction expressed as a fraction. If a given probability and M_w of 7.5 is used in Eq. 10, a plot of *CRR* vs. V_{s1} can be produced for a given probability. Fig. 3 provides a plot of *CRR* vs. N'_{120} for M_w 7.5 for various P_L values proposed by Rollins et al. [29].

The new probabilistic triggering curves with liquefaction probabilities of 15% to 85% are plotted in Fig. 4(a) with solid lines along with similar curves developed by Cao et al. [18] with dashed lines to draw a distinct comparison between the two triggering procedures. For lower values of V_{s1} (around 150 m/s), the *CRR* for the new 50% probability of liquefaction curve is about 0.10 while it is only 0.04 for the Cao et al. [18] curves. This adjustment produces much better agreement with observed field performance. This higher *CRR* value at small velocities are also more typical of that predicted by the V_s-based triggering curves developed by Kayen et al. [11]. Case history data points where gravels did not liquefy in Fig. 3 from the Port of Wellington and ports in Argostoli, Italy, have had a significant effect in constraining the lower branch of the triggering curves to move upwards. Likewise, the triggering curves at the higher range of V_{s1} values have been tightened relative to the curves developed by Cao et al. [3] owing to additional "no liquefaction" data points from Chengdu, L'Aquila, Italy and Valdez, Alaska. Additional data points would certainly be desirable to define the shape of the curve better in this range of V_{s1} values.

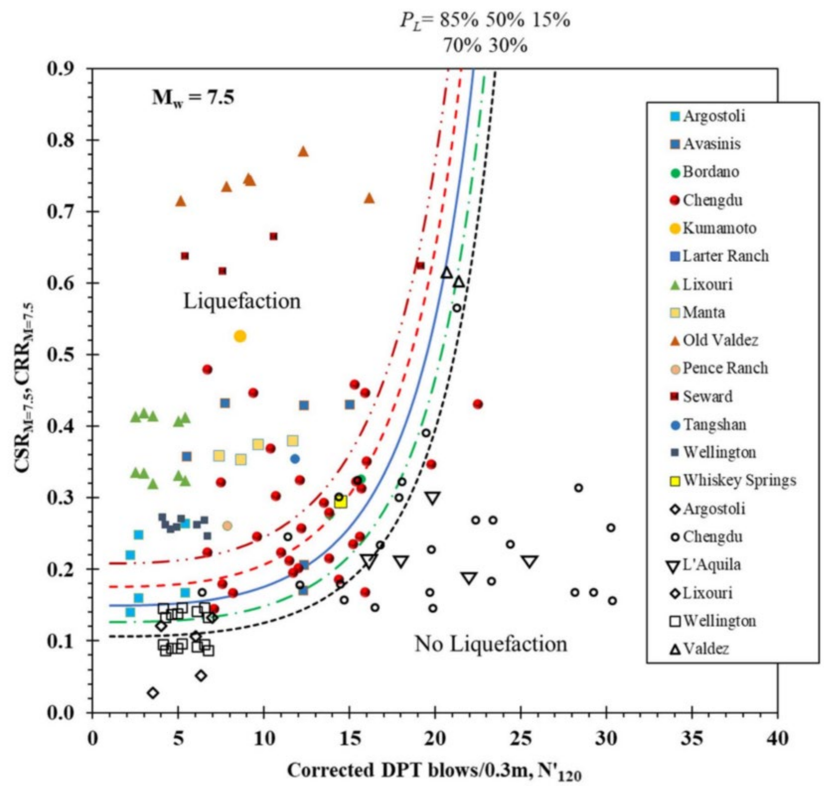

Figure 2. Plot of *CRR* vs. *N'*$_{120}$ for a M_w 7.5 earthquake with various probabilities of liquefaction based on expanded DPT-based database proposed by Rollins et al. [28].

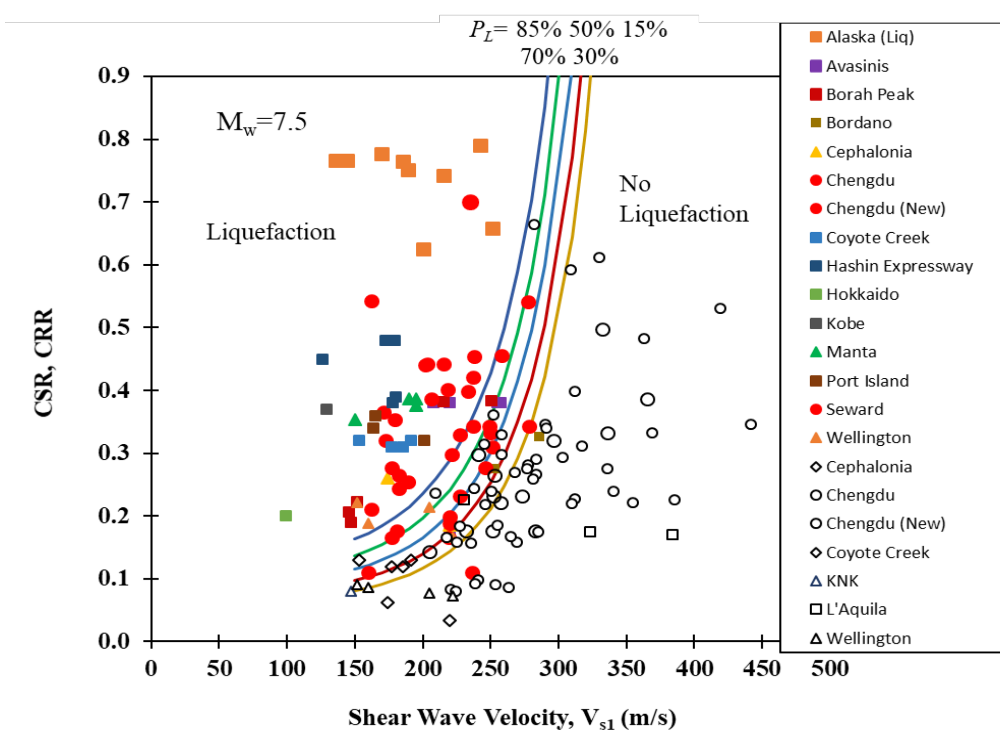

Figure 3. Plot of CRR vs. V_{s1} for a M_w 7.5 earthquake with various probabilities of liquefaction based on expanded Vs -based database collected by Rollins et al. [29].

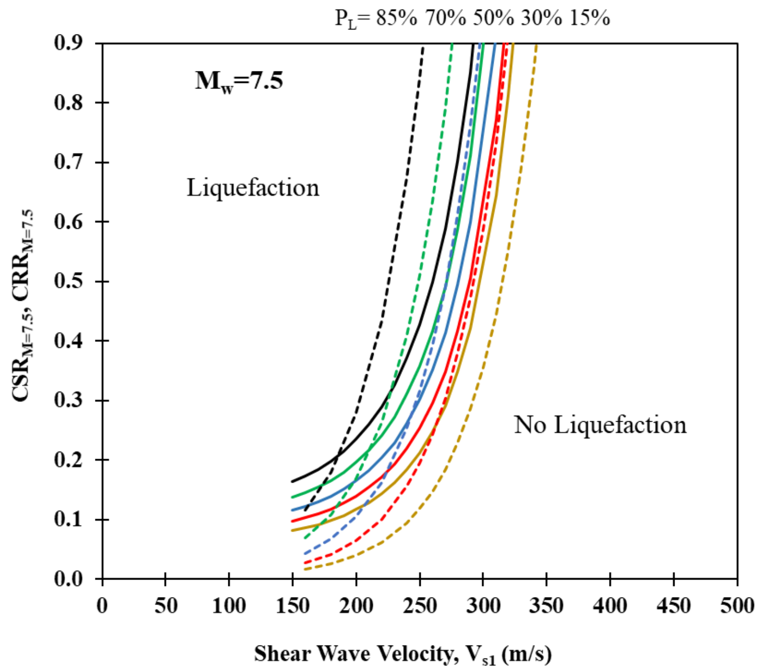

(a)

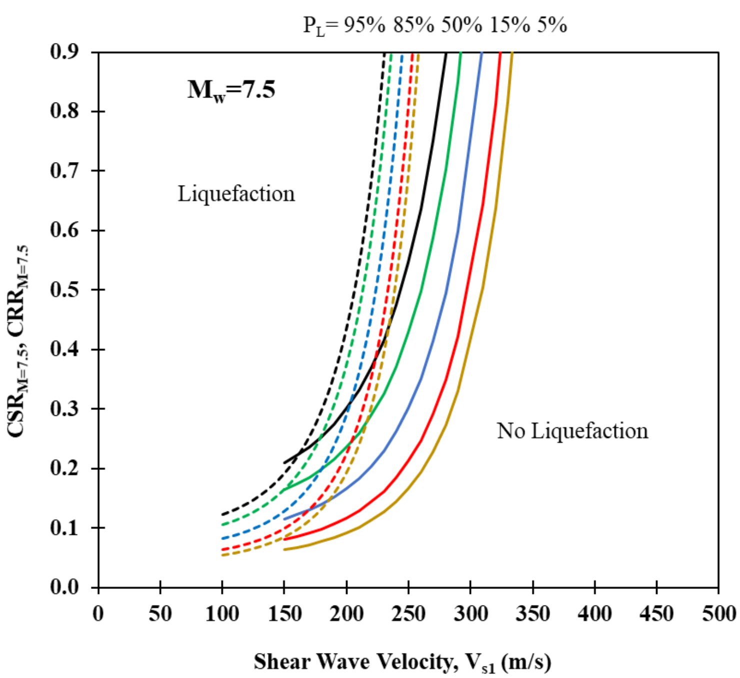

(b)

Figure 4. Revised liquefaction triggering curves from this study (solid lines) (a) relative to triggering curves originally proposed by Cao et al. [18] (dashed lines) and (b) relative to triggering curves proposed by Kayen et al. [11] for sands (dashed lines).

As shown in Fig. 4(a), for V_{s1} values above 200 m/s, the P_L = 50% curve for the new regression is very similar to that for the Cao et al. [18] regression. However, the addition of new liquefaction points has pulled the new P_L=85% curve to the right while the addition of no-liquefaction data points has pulled the new P_L=15% curve to the left, relative to the Cao et al. [18] curves. Moving the new P_L=15% curve to the left is important because this curve is often recommended for deterministic evaluations [11]. However, the slope of the new set of curves from this study remains almost the same as for the Cao et al. [18] curves. Overall, the spread between the triggering curves for various probabilities of liquefaction is substantially reduced for the new triggering curves relative to the Cao et al. [18] curves. This result is consistent with the concept that the increased number of data points reduces the uncertainty that develops when an individual data point plots in an unexpected position. Furthermore, the addition of data points where liquefaction did not occur has helped constrain the triggering curves on the “no liquefaction side” in critical locations.

Fig. 4 (b) provides a comparison is provided between the newly developed triggering curves for gravel and the curves developed by Kayen et al. [11] for sand. To plot the triggering curves for Kayen et al. [11], an average effective vertical stress of 100 kPa, and fines content of 6% has been assumed to keep the values within a reasonable range. Although the probabilistic liquefaction triggering curves for gravel developed in this study are similar to those for sands [11] at lower V_{s1} values typical of looser gravels, the curves diverge as V_{s1} increases. For example, V_{s1} equals 275 m/s for the proposed P_L = 50% curve for gravel in this study at a CRR of 0.5 in comparison with a V_{s1} of only 225 m/s for the P_L = 50% curve for sand proposed by Kayen et al. [11]. This indicates that the probabilistic triggering curves for gravels from this study shift to the right relative to similar curves developed for sands as V_{s1} increases. This result indicates that gravels can still liquefy at V_{s1} values that would be high enough to preclude liquefaction in a sand. This does not mean that gravels are more or less likely to liquefy than sand, it simply means that for a comparable level of shaking, a higher V_{s1} is necessary to obtain the same probability of liquefaction for a sandy gravel as that for a sand. This result is consistent with liquefaction case histories in gravels reported by several investigators [15, 18, 30, 31] where V_s-based triggering curves for sands would have incorrectly predicted no liquefaction. Similar results have also been observed in laboratory testing (e.g. [32, 33]).

VI. DEVELOPMENT OF MAGNITUDE SCALING FACTORS

Most liquefaction triggering curves adjust the *CSR* for earthquake magnitude using a Magnitude Scaling Factor (MSF) to obtain an equivalent *CSR* for a M_w of 7.5 using the equation,

$$CSR_{M=7.5} = CSR/MSF \tag{11}$$

As a part of the present study, we have developed new *MSF* models specifically for gravelly soils that will simplify liquefaction evaluation at gravel sites for different magnitude earthquakes; however, more data from other earthquakes would be desirable to improve the data set. The *MSF* for triggering analyses using the DPT blow counts can be computed as a function of magnitude with the best-fit exponential equation,

$$MSF = 7.258exp(-0.264M_w) \tag{12}$$

Likewise, the *MSF* for triggering analyses using V_{s1} can be computed as a function of magnitude with the best-fit exponential equation.

$$MSF = 10.667exp(-0.316M_w) \tag{13}$$

These *MSF* curves are plotted and compared with several other *MSF* vs. M_w curves in Fig. 5. It can be observed that the *MSF* curves developed for gravelly soil fall about mid-way between the *MSF* vs. M_w curves for sand suggested by Idriss and endorsed by the NCEER/NSF liquefaction workshop [10] at the high end and the Kayen et al. [11] curve at the low end. Hence, the proposed *MSF* curves for gravel appear to be reasonably consistent with existing *MSF* curves for sands.

Based on these *MSF* equations, the *CSRs* for all the case history data points have been converted to CSRs at M_w = 7.5 and plotted with the newly developed triggering curves as shown in Figs. 2 and 3. Generally, the data points fall on the correct sides of the P_L = 50% curves for liquefaction and no liquefaction.

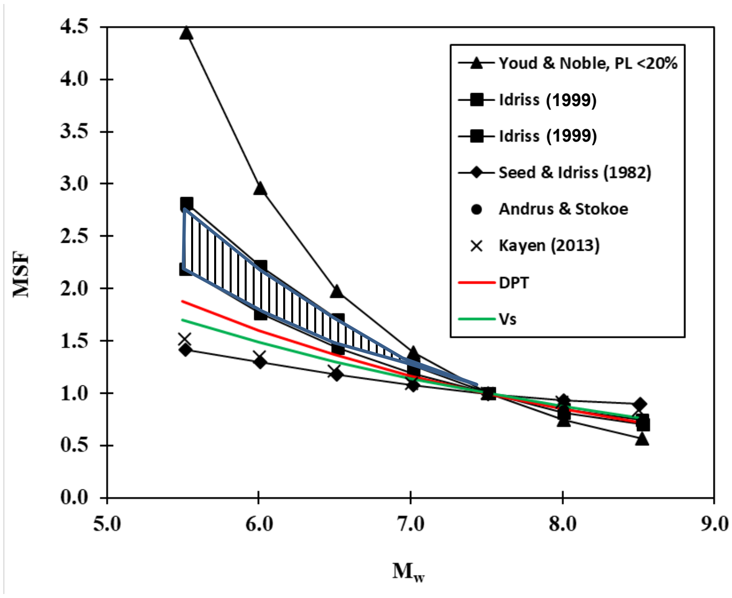

Figure 5. Comparison of *MSF* curves from logistical regression analysis of gravel liquefaction case histories based on *Vs* and DPT triggering curve with *MSF* curves proposed previously for sand [28, 29].

VII. COMPARISION OF BPT AND DPT LIQUEFACTION FACTOR OF SAFETY

To provide a comparison between the liquefaction factor of safety computed by the Becker Penetrometer (BPT) and the Dynamic Cone Penetrometer (DPT) in the field, we performed DPT test holes within a few meters of locations where BPT tests were previously performed [14,34] at liquefaction case history sites in Idaho subjected to the M_w 6.9 1985 Borah Peak Earthquake. Four DPT tests were performed at the Larter Ranch and Pence Ranch sites, while two were performed at the Whiskey Springs site. Peak ground accelerations at these sites were between 0.4 and 0.5 g. The critical liquefaction layers for the DPT were very similar to those identified by the BPT holes. For the critical layers in each hole at each site, the average Cyclic Stress Ratio (CSR) was computed using Eqs. 1 and 11. The Cyclic Resistance Ratio (CRR) was computed for the DPT holes using Eq. 9. However, the CRR for the BPT holes was based on the equivalent SPT N_{60} value reported by Andrus [14, 34] that was obtained using a correlation between equivalent sand SPT N_{60} value and the BPT N_{BC} developed by Harder and Seed [5]. With the equivalent sand SPT N_{60}, the $(N_1)_{60}$ was determined and the CRR calculated using the Idriss and Boulanger [24] approach. Table 1 provides a summary of the average CSR, CRR and factor of safety against liquefaction (FS_L) for the sites at Larter Ranch, Pence Ranch, and Whiskey Springs obtained from the companion DPT and BPT holes. Although there is some variation in the CRR as would be expected for natural soil deposits, the average percent difference in the FS_L from the DPT and BPT methods for the three sites range from only 4% to 17% with an overage average of 11%. The worst agreement was for the Whiskey Springs site where only two holes were available for comparison. Considering that both methods were developed from completely different data set with different methods for normalizing blow counts, this close agreement provides confirmation of the validity of both methods.

TABLE 1

Comparison of DPT- and BPT-based Liquefaction Assessment at 1985 Borah Peak Gravel Liquefaction Sites

Summary of DPT Testing				Summary of BPT Testing				
Site	Avg. CSR	Avg. CRR	Avg. FS_L	Site	Avg. CSR	Avg. CRR	Avg. FS_L	% Difference in BPT and DPT FS_L
Larter Ranch	0.26	0.11	0.42	Larter Ranch	0.26	0.10	0.38	10
Pence Ranch	0.28	0.12	0.43	Pence Ranch	0.28	0.115	0.41	4
Whiskey Springs	0.28	0.175	0.63	Whiskey Springs	0.28	0.15	0.54	17
Average			0.49	Average			0.44	11

VIII. SUMMARY AND CONCLUSIONS

In this study, probabilistic liquefaction-triggering curves for gravelly soils based on the Dynamic Cone Penetration (DPT) test blow count (N'_{120}) and shear-wave velocity (Vs) presented that can be used for liquefaction evaluation of gravelly soils for a wide range of earthquake magnitudes, tectonic settings, and geological environments. These curves are a significant step forward compared to those developed by Cao et al. [3,19], as the total number of data points has increased significantly. The N'_{120} and Vs1 data were compiled from various sites around the world where liquefaction or no liquefaction case histories of gravelly soils were observed during several earthquake events in the past. The expanded data set consisted of 174 Vs data points and 137 DPT data points from 17 different earthquakes in 10 different countries in a variety of geological environments. Additional case histories from future events should help improve the triggering curves as we move forward. Comparisons were also made between the liquefaction factor of safety obtained from the BPT and DPT at gravel liquefaction sites from the 1985 Borah Peak earthquake. Based on the results of the field studies and data analysis performed in this study, the following conclusions were drawn:

1. The increased number of liquefaction and no-liquefaction data points in the expanded data set better constrain the probabilistic liquefaction-triggering curves. Relative to the Cao et al. [26] curves for V_s and the Cao et al. [3] curves for DPT, this shifted the P_L = 85% curve to the right and P_L = 15% curve to the left. The reduction in the range between the P_L = 85% and 15% curves indicate a considerable decrease in uncertainty, because false negative data points have less impact on the expanded data set. Shifting the P_L = 15% curve to the left is significant because this probability curve has been recommended for deterministic analyses (e.g. [11]).
2. At lower V_{s1} values (≈150 m/s) and DPT blow counts less than 7, typical of looser gravels, the proposed triggering curves for gravel in this study start at a higher range of CSRs compared to the curves developed by Cao et al. [3, 19]. This modification was necessary to produce agreement with the no-liquefaction points from the field case histories and brought the CSR values in line with the V_{s1} values for sand as predicted by the Kayen et al. [11] probability curves.
3. Simplified *MSF* versus moment magnitude M_w equations were developed exclusively for gravel liquefaction. The *MSF* versus M_w curves plot about midway between similar curves proposed for sand. These results suggest that the effect of magnitude on liquefaction resistance is similar, but slightly different, for both sands and sandy gravels.
4. Although the new probabilistic triggering curves for gravel are similar to those for sands [18] at low V_{s1} values typical of loose gravels (≈150 m/s), they shift to the right as V_{s1} values increase. This indicates that gravels can still liquefy at values that would preclude liquefaction for sands. Therefore, using V_s-based triggering curves for sand when encountering gravels could incorrectly estimate gravel susceptible to liquefaction as being non-liquefiable.
5. The factor of safety against liquefaction computed using the DPT and BPT methods at gravel liquefaction sites in the 1985 Borah Peak Earthquake were within 11% of one another despite the fact that the liquefaction resistance for these two methods are based on entirely different data sets and normalization procedures. This close agreement between these two methods tends to validate the reliability of both methods.

IX. ACKNOWLEDGEMENTS

Funding for this study was provided by grant G16AP00108 from the US Geological Survey Earthquake Hazard Reduction Program and grants CMMI-1663546 and CMMI-1663288 from the National Science Foundation. This funding is gratefully acknowledged. This work is also part of a Research Project funded by ReLUIS (University Network of Seismic Engineering Laboratories) Consortium 2019-2021, WP 16 Geotechnical Engineering, Task 16.1 Site response and liquefaction. However, the opinions, conclusions and recommendations in this paper do not necessarily represent those of the sponsors. We also express sincere appreciation to L. Minarelli for help in arranging access for geophysical surveys at sites in Italy and to G. Athanasopoulos for arranging access for these tests at sites in Cephalonia, Greece.

X. REFERENCES

[1] Seed, H. B., Martin, P. P. and Lysmer, J. 1976. "The generation and dissipation of pore water pressure changes during soil liquefaction". *Journal of the Geotechnical Engineering Division*, 102(4), 323-346.
[2] Roy, J. and Rollins, K.M. (2022). "Effect of hydraulic conductivity and impeded drainage on the liquefaction potential of gravelly soils." Canadian Geotechnical J., Canadian Science Publishing, 58(11) pp. 1950-1968.
[3] Cao, Z., Youd, T., and Yuan, X. 2013. "Chinese Dynamic Penetration Test for liquefaction evaluation in gravelly

soils."*J. Geotech. Eng.*, 10.1061/(ASCE)GT.1943-5606.0000857.

[4] DeJong, J.T., Ghafghazi, M., Sturm, A.P., Wilson, D.W., den Dulk, J., Armstrong, R.J., Perez, A., and Davis, C.A. 2017. "Instrumented Becker Penetration Test. I: Equipment, Operation, and Performance." *J. Geotech. Eng.*, doi.org/10.1061/(ASCE)GT.1943-5606.0001718.

[5] Harder, L.F., Jr., and Seed, H.B. 1986. "Determination of penetration resistance for coarse-grained soils using the Becker Hammer Drill." College of Engineering, University of California, Berkeley, Calif. Rep. No. UCB/EERC-86/06. May 1986.

[6] Harder, L.F. 1997. "Application of the Becker Penetration Test for evaluating the liquefaction potential of gravelly soils."*NCEER Workshop on Evaluation of Liquefaction Resistance*, held in Salt Lake City, Utah.

[7] ASTM. 2018. Standard test method for use of the dynamic cone penetrometer in shallow pavement applications. ASTM D6951/D6951M-18. West Conshohocken, PA: ASTM.

[8] British Standard 2012, Geotechnical investigation and testing — Field testing — Part 2: Dynamic probing BS EN ISO 22476-2:2005+A1:2011

[9] Boulanger, R.W. and Idriss, I.M. 2014. "CPT and SPT based liquefaction triggering procedures." Center of Geotechnical Modeling, Univ. of California-Davis, Report No. UCD/CGM-14/01.

[10] Youd, T.L., Idriss, I.M., Andrus, R.D., Arango, I., Castro, G., Christian, J.T., Dory, R., Finn, W.D.L., Harder, L.F., Hynes, M.E., Ishihara, K., Koester, J.P., Liao, S.S.C., Marcuson, W.F., Martin, G.R., Mitchell, J.K., Moriwaki, Y., Power, M.S., Robertson, P.K., Seed, R.B., and Stokoe, K.H. 2001. "Liquefaction resistance of soils: Summary Report from the 1996 NCEER and 1998 NCEER/NSF Workshops on evaluation of liquefaction resistance of soils."*J. Geotech. Eng.*, 10.1061/(ASCE)1090-0241(2001)127:10(817).

[11] Kayen, R., Moss, R.E.S., Thompson, E.M., Seed, R.B., Cetin, K.O., Der Kiureghian, A., Tanaka, Y., and Tokimatsu, K. (2013). "Shear-wave velocity-based probabilistic and deterministic assessment of seismic soil liquefaction potential." *J. Geotech. Eng.*, doi.org/10.1061/(ASCE)GT.1943-5606.0000743.

[12] Stokoe, K. H. II, Wright, S. G., Bay, J. A., and Roesset, J. M. 1994."Characterization of geotechnical sites by SASW method," ISSMFE, Technical Committee #10 for XIII ICSMFE, Geophysical Characterization of Sites, A. A. Balkema Publishers/Rotterdam & Brookfield, Netherlands,15–25.

[13] Andrus, R.D., and Stokoe, K.H., II 2000. "Liquefaction resistance of soils from shear-wave velocity." *J. Geotech. Eng.,* 10.1061/(ASCE)1090-0241(2000)126:11(1015).

[14] Andrus, R.D. 1994. "In-situ characterization of gravelly soils that liquefied in the 1983 Borah Peak earthquake." *Ph.D. Dissertation*, Civil Engineering Dept., Univ. of Texas at Austin, 579 pp.

[15] Chang, W.J. 2016. "Evaluation of liquefaction resistance for gravelly sands using gravel content-corrected shear-wave velocity." *J. Geotech. Eng.*, 10.1061/(ASCE)GT.1943-5606.0001427.

[16] Ohta, Y. and Goto, N. 1978. "Physical background of the statistically obtained S-wave velocity equation in terms of soil indexes." *ButsuriTanko(Geophysical Exploration),* Tokyo, Japan, 31(1), 8-17 (In Japanese).

[17] Rollins, K.M., Evans, M., Diehl, N. and Daily, W. 1998b. "Shear modulus and damping relationships for gravels." *J. Geotech. and Geoeviron. Eng.*., ASCE, 124(5) p. 396-405.

[18] Cao, Z., Youd, T.L., and Yuan, X. 2011. "Gravelly soils that liquefied during 2008 Wenchuan, China Earthquake, Ms=8.0." *Soil Dynamics and Earthquake Engineering*, 31(8), 1132-1143.

[19] Chen, L. Yuan, X., Cao, Z. Sun, R. Wang, w., and Liu H. 2018. "Characteristics and Triggering Conditions for Naturally Deposited Gravelly Soils that Liquefied following the 2008 Wenchuan M_w 7.9 Earthquake, China." Earthquake Spectra, 34(3) p. 1091-1111

[20] Seed, H. B., and I. M. Idriss. 1971. "Simplified procedure for evaluating soil liquefaction potential." J. Soil Mech. Found. Div. 97 (9): 1249–1273 https://doi.org/10.1061/JSFEAQ.0001662.

[21] Golesorkhi, R. 1989. "Factors influencing the computational determination of earthquake-induced shear stresses in sandy soils." PhD dissertation, University of California, Berkeley, California.

[22] Idriss, I.M. 1999. "An update to the Seed-Idriss simplified procedure for evaluating liquefaction potential." *Procs. TRB Workshop on New Approaches to Liquefaction*, Publication No. FHWA-RD-99-165, Federal Highway Administration.

[23] Worden, C. B., Wald, D. J., Allen, T. I., Lin, K., and Cua, G. 2010. "Integration of macroseismic and strong-motion earthquake data in ShakeMap for real-time and historic earthquake analysis." USGS website, http://earthquake.usgs.gov/earthquakes/shakemap/.

[24] Idriss, I. M., & Boulanger, R. W. (2008). "Soil liquefaction during earthquakes." Report No. MNO-12. Oakland, CA: Earthquake Engineering Research Institute.

[25] Cao, Z., Yuan, X., Youd, T.L., and Rollins, K.M. 2012. "Chinese Dynamic Penetration tests (DPT) at liquefaction sites following 2008 Wenchuan Earthquake." *Proc., 4th Int. Conf. on Geotechnical and Geophysical Site Characterization, Taylor & Francis Group, London*, 1499-1504.

[26] Seed, H.B., Tokimatsu, K., Harder, L.F., and Chung, R.M. 1985. "Influence of SPT procedures in soil liquefaction resistance evaluations." *J. Geotech. Eng.*, 10.1061/(ASCE)0733-9410(1985)111:12(1425).

[27] Sykora, D. W. 1987. ''Creation of a data base of seismic shear wave velocities for correlation analysis.'' *Geotech. Lab. Misc. Paper GL-87-26*, U.S. Army Engr. Waterways Experiment Station, Vicksburg, Miss.

[28] Rollins, K.M., Roy, J., Athanasopoulos-Zekkos, A., Zekkos, D., Amoroso, S., Cao, Z. (2021). "New dynamic cone penetration test-based procedure for liquefaction triggering assessment of gravelly soils." J. Geotechnical and Geoenvironmental Engrg. ASCE, 147(12), 13 p.

[29] Rollins, K.M., Roy, J., Athanasopoulos-Zekkos, A., Zekkos, D., Amoroso, S., Cao, Z., Millana, G., Vassallo, M., Di Giulio, G. (2022). "A New V_s-Based Liquefaction Triggering Procedure for Gravelly Soils." J. Geotechnical and Geoenvironmental Engrg., 148(6), 15 p. ASCE DOI: 10.1061/(ASCE)GT.1943-5606.0002784

[30] Rollins, K.M., Amoroso, S., Milan, G., Minerelli, L., Vassallo, M., Di Giulio, G. (2020). “Gravel liquefaction assessment using the dynamic cone penetration test based on field performance from the 1976 Friuli earthquake.” J. Geotechnical & Geoenvironmental Engrg., ASCE, 146(6).

[31] Athanasopoulos-Zekkos, A., Zekkos, D., Rollins, K.M., Hubler, J., Higbee, J., Platis, A. 2019. “Earthquake performance and characterization of gravel-size earth fills in the ports of Cephalonia, Greece, following the 2014 Earthquakes.” Earthquake Geotechnical Engineering for Protection and Development of Environment and Constructions, Procs. 7th Intl. Conf. on Earthquake Geotechnical Engineering, Taylor and Francis, p. 1212-1219.

[32] Hubler, J., Athanasopoulos-Zekkos, A., and Zekkos, D. 2018 “Monotonic and cyclic simple shear response of gravel-sand Mixtures”, *Soil Dynamics and Earthquake Engineering, Vol 115, pp. 291-304, Dec 2018,*

[33] Hubler, J., Athanasopoulos-Zekkos, A., and Zekkos, D. 2017. “Monotonic, cyclic and post-cyclic simple shear response of three uniform gravels in constant volume conditions”, *J. Geotech. and Geoenviron Eng.* ASCE, Washington, DC, 143(9)

[34] Andrus, R.D. 1986 “Subsurface investigations on a liquefaction induced lateral spread Thousand Springs Valley, Idaho: Liquefaction recurrence and a case history in Gravel, M.S. Thesis, Dept. of Civil Engineering, Brigham Young Univ., 118 p.

XI. AUTHOR BIOGRAPHIES

Kyle M. Rollins, Ph.D.
Professor of Civil Engineering
Brigham Young University
430 EB
Provo, UT 84604
801-422-6334 / rollinsk@byu.edu

Bio-sketch

Kyle Rollins received his BS degree from Brigham Young University and his Ph.D. from the University of California at Berkeley. After working as a geotechnical consultant, he joined the Civil Engineering faculty at BYU in 1987, following his father who was previously a geotechnical professor. He has supervised more than 130 graduate students and published over 200 papers. His research has involved liquefaction assessment of gravels, lateral resistance of piles and pile groups, passive resistance of bridge abutments, lightweight cellular concrete for retaining structures, and various soil improvement techniques. His studies typically involve full-scale testing to determine “ground truth” behavior. Prof. Rollins was the chair of the Geo-Institute technical committee on soil improvement, and ASCE has recognized his work with the Huber research award, the Wellington prize, and the Wallace Hayward Baker award. In 2009, he was the Cross-Canada Geotechnical lecturer for the Canadian Geotechnical Society, and he is the Cross-USA lecturer for the ASCE Geo-Institute for this coming year. He received the Utah Governor’s medal for science and technology and the Osterberg Innovation Award from the Deep Foundation Institute.

Jashod Roy
Geotechnical Engineer
Kiewit Engineering, Inc.
8900 Renner Blvd
Lenexa, KS – 66219
385-349-6070 / Jashod.roy@gmail.com

Bio-sketch

Jashod Roy received his B.E. in civil engineering from Jadavpur University in India in 2014. After completion of his B.E., he worked for Fluor Corporation during 2014-2015 as a structural engineer. In 2017, he completed his M.Tech from IIT Bombay with a specialization in geotechnical engineering. Further, he received his Ph.D. from Brigham Young University in 2022 in the field of Geotechnical Engineering under the supervision of Prof. Kyle Rollins. His research during his academic years primarily involved analysis and design of combined pile raft foundation under earthquake loading, liquefaction assessment of gravelly soils based on in-situ tests, and numerical studies. Currently, he is working as a geotechnical engineer for Kiewit in Omaha, Nebraska.